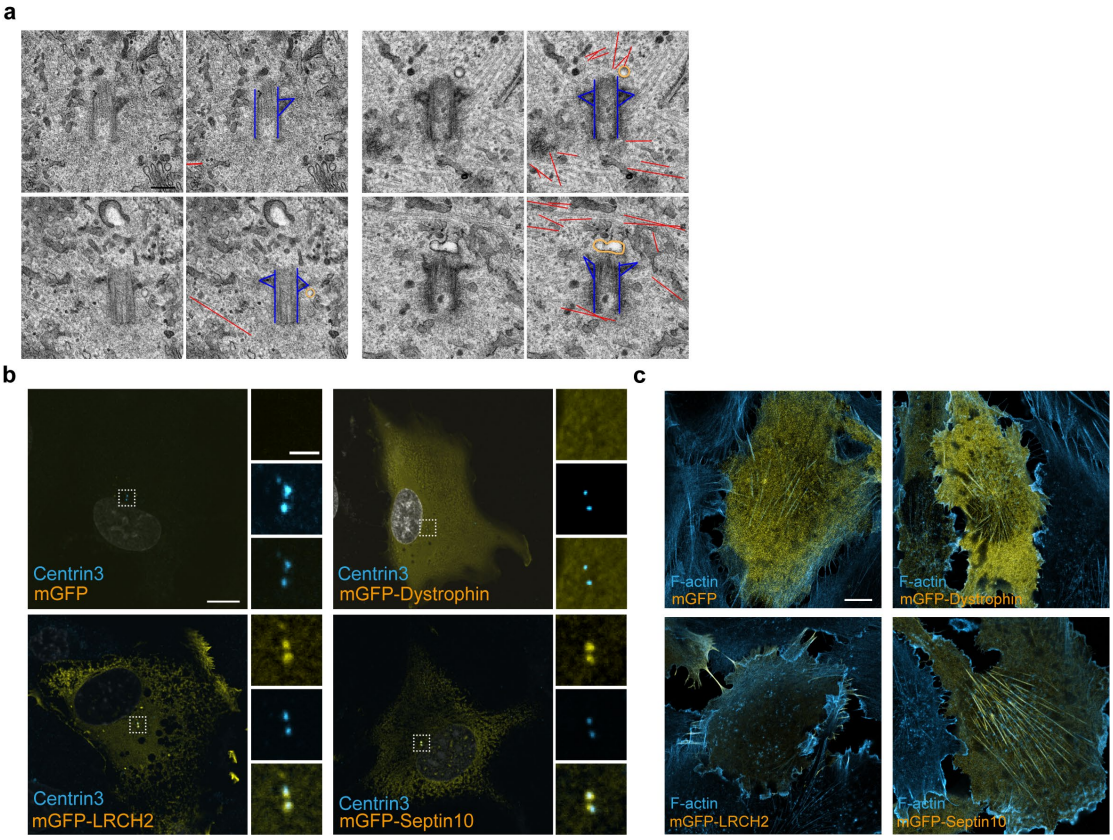

Supplementary Fig. 1 | Screening for mediators of centrosomal branched actin in ciliogenesis regulation.

a, Transmission electron microscopy images showing the distribution of F-actin (red) and ciliary vesicles (yellow) around the centrosome (blue) in cells expressing mEmerald-PACT or mEmerald-PACT-VCA. Scale bar: 200 nm. **b,** Centrosomal localization of multiple actin-microtubule crosslinking proteins. Centrin3 marks centrosomes. Scale bars: 10 µm (2 µm for insets). **c,** Confocal images of candidate proteins (yellow) with F-actin (blue). Scale bar: 10 µm.

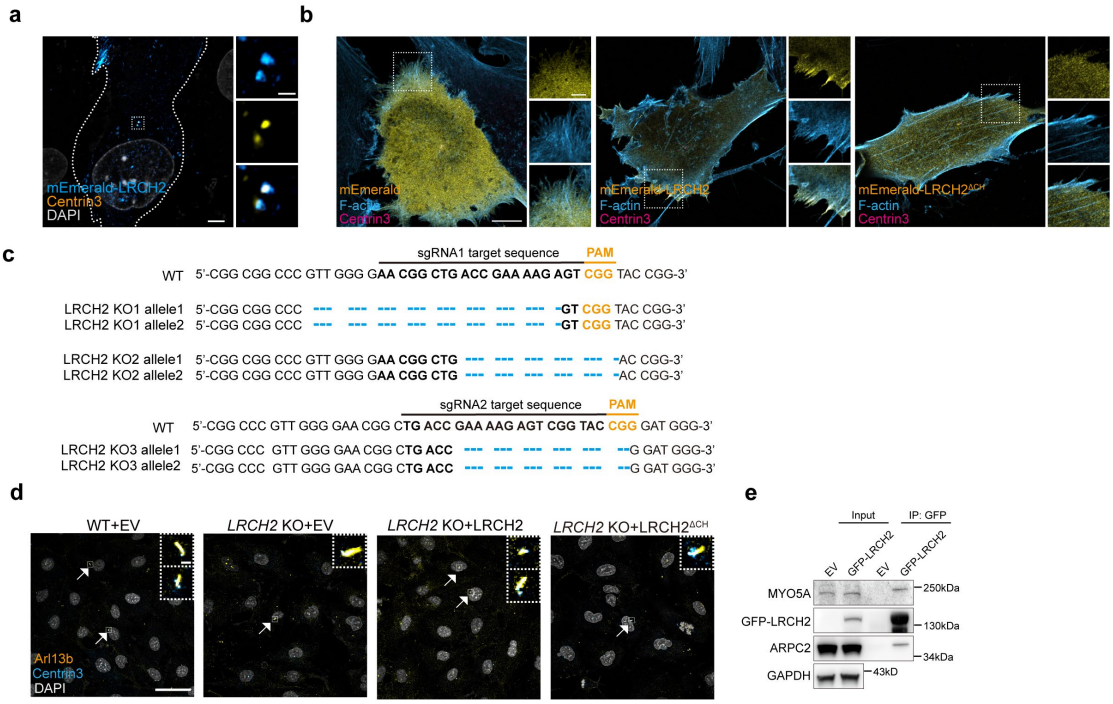

Supplementary Fig.2 | Re-expressing LRCH2 in LRCH2 KO cells.

a, Immunofluorescence of Centrin3 (yellow) in cells expressing mEmerald-LRCH2. Scale bars: 100 µm (1 µm for insets). **b,** Immunofluorescence images of Centrin3 (pink) in cells expressing mEmerald, mEmerald-LRCH2 or mEmerald-LRCH2$^{\Delta CH}$ (yellow), with F-actin marked by phalloidin (blue). Scale bar: 10 µm (3 µm for insets). **c,** Genotyping of *LRCH2* KO cells. **d,** Immunofluorescence images of cilia (Arl13b, yellow) in wild-type (WT) and *LRCH2* knockout (KO) RPE1 cells expressing full-length LRCH2 or LRCH2 lacking the CH domain (LRCH2$^{\Delta CH}$), following 3 h of serum starvation. Scale bar: 50 µm (2 µm for insets). **e,** IP analysis of GFP-LRCH2 and MYO5A and ARPC2, using an anti-GFP antibody.

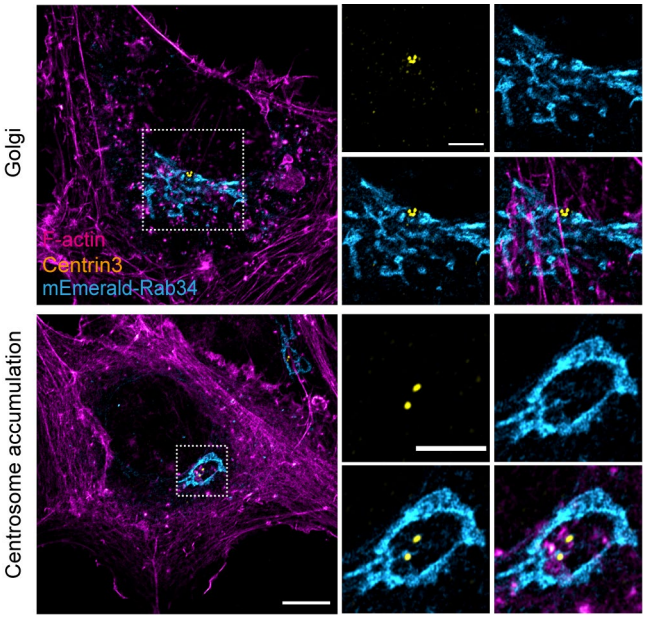

Supplementary Fig. 3 | Localization pattern of Rab34.

Immunofluorescence images of Centrin3 (yellow) in cells expressing mEmerald-Rab34 (blue), with F-actin marked by phalloidin (pink). Scale bars: 10 μm (5 μm for insets)

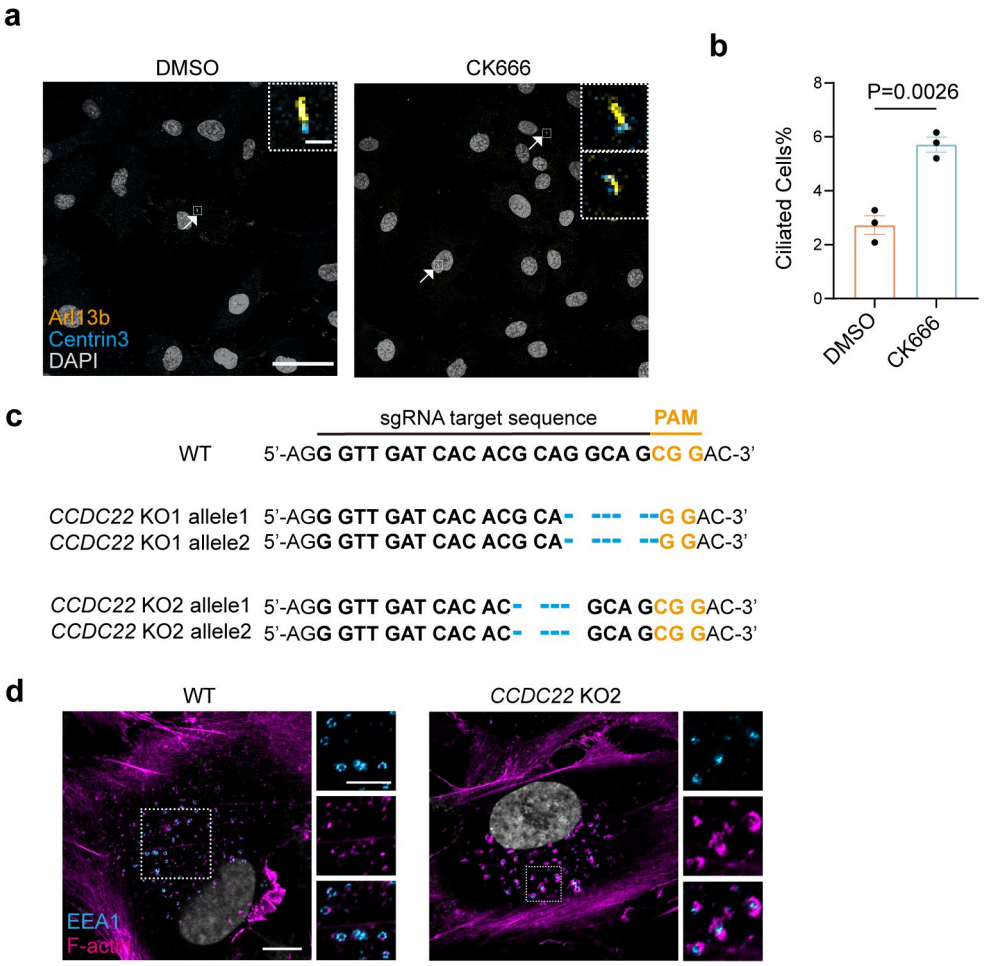

Supplementary Fig. 4 | CCDC22 deficiency impairs ciliogenesis.

a, Immunofluorescence staining of cilia (marked by Arl13b, yellow) and centrosomes (marked by Centrin3, blue) in RPE1 cells treated with the branching actin inhibitor CK666 (200 μM) for 12 h. Scale bars: 20 μm (1 μm for insets). **b,** Quantification of the percentage of ciliated cells in **a.** Data are shown as mean ± s.e.m.; n = 3 independent experiments. Statistical significance was determined by an unpaired two-tailed t-test. **c,** Genotyping of *CCDC22* KO cells. **d,** Immunofluorescence images of the endosomal marker EEA1 (blue) in WT and *CCDC22* KO cells, with F-actin marked by phalloidin (pink). Scale bars: 10 μm (5 μm for insets).

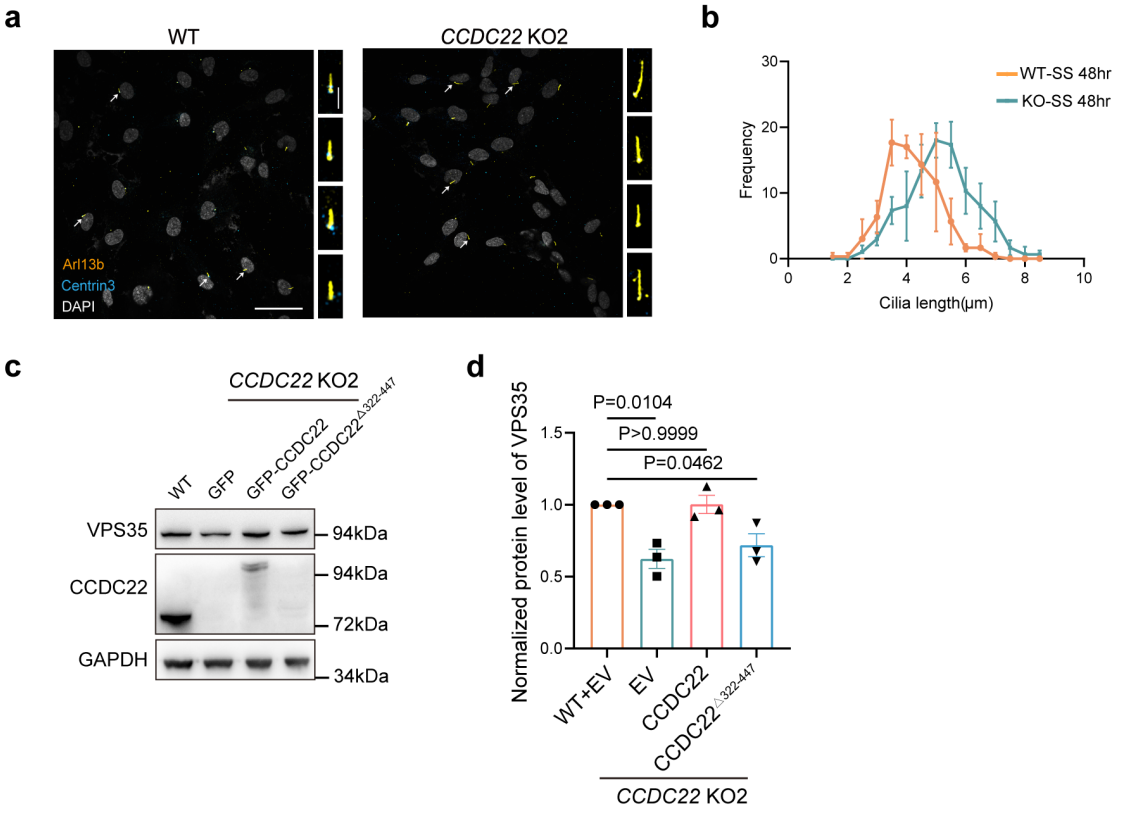

Supplementary Fig.5 | Ciliogenesis is impaired in *CCDC22* KO cells.

a, Immunofluorescence images of cilia (Arl13b, yellow) and centrosome (Centrin3, blue) in WT and *CCDC22* KO cells after 48 h of serum starvation. **b,** Distribution of cilium length in WT and *CCDC22* KO cells after 48 h of serum starvation. Data are presented as mean ± s.e.m.; n = 3 independent experiments. **c,** Immunoblot analysis of the recycling endosome protein VPS35 in WT cells, *CCDC22* KO cells, and *CCDC22* KO cells reconstituted with either full-length CCDC22 or the CCDC22$^{\Delta 322\text{-}447}$ mutant. **d,** Quantification of protein level of VPS35 in **c**, normalized by GAPDH. Data are shown as mean ± s.e.m.; n = 3 independent experiments. Statistical significance was determined by one-way ANOVA with multiple comparisons.

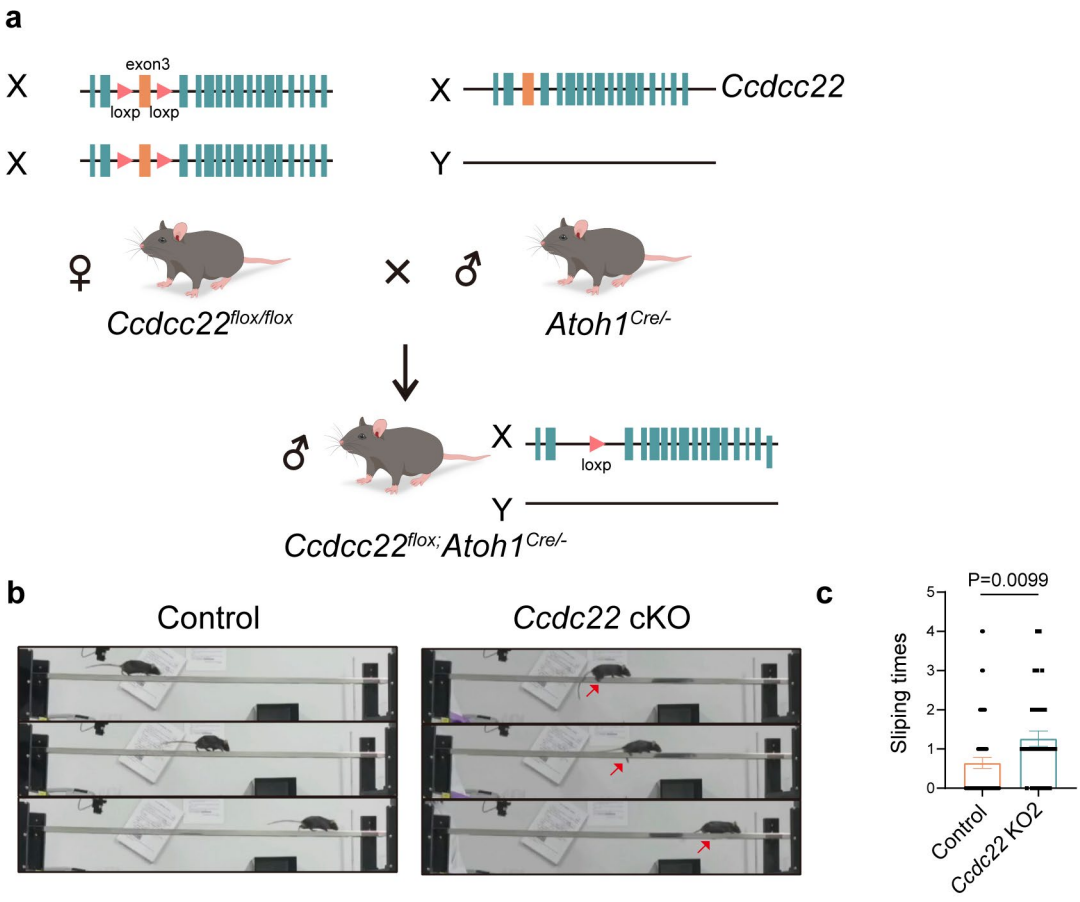

Supplementary Fig. 6 | Generation of GCP-specific *Ccdc22* knockout mice and balance beam test.

a, Schematic of the breeding strategy used to generate GCP-specific *Ccdc22* knockout mice via *Atoh1-Cre*-mediated recombination. **b,** Representative images of mice crossing the balance beam at 2 months of age; red arrows indicate paw slips. **c,** Quantification of slipping times in **b,** data are presented as mean ± s.e.m.; n = 21 for control mice, n = 23 for *Ccdc22* cKO mice. Statistical significance assessed by an unpaired two-tailed t-test.

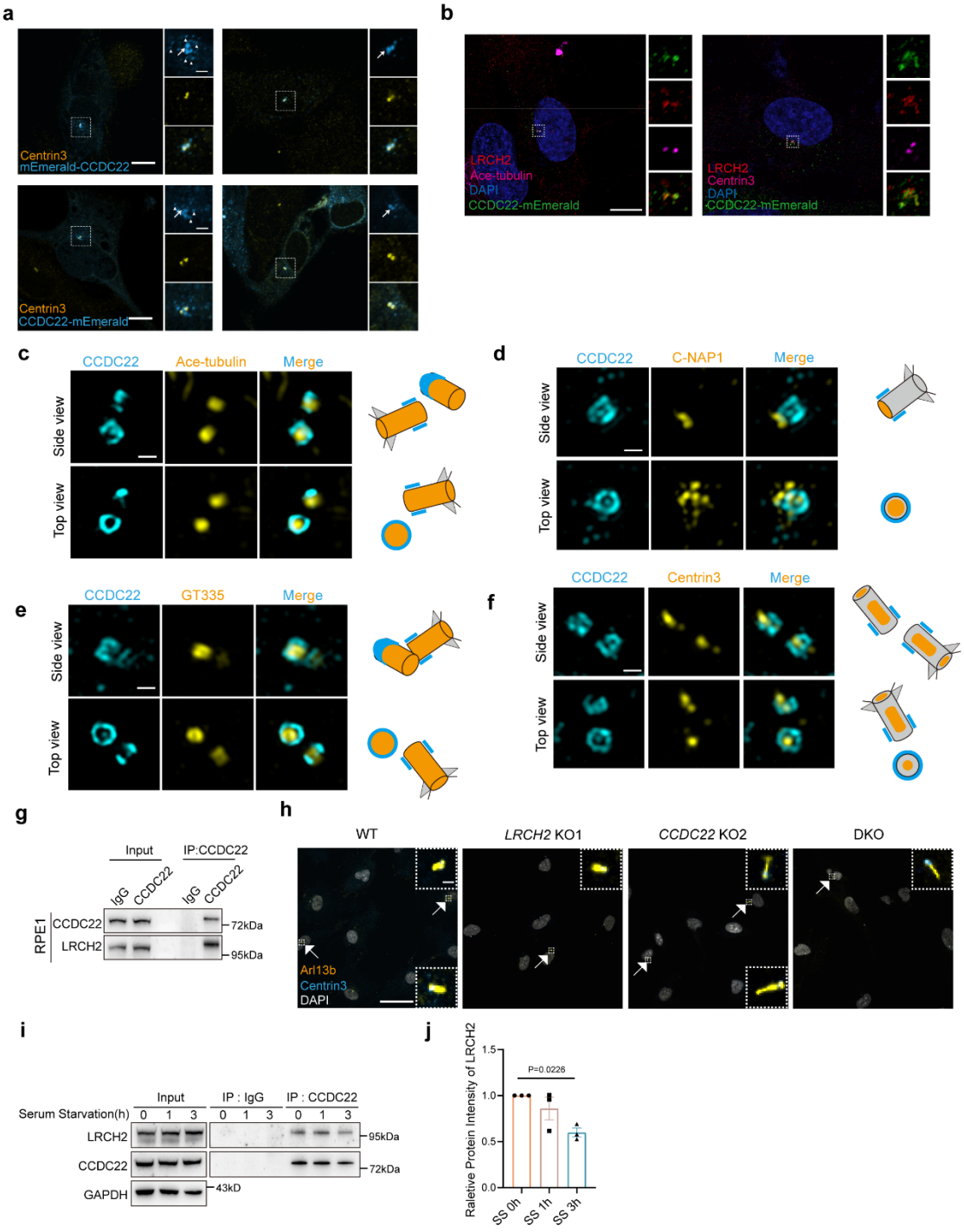

Supplementary Fig. 7 | CCDC22 is also a centrosome protein and interacts with LRCH2. **a,** Confocal microscopy images of exogenous CCDC22 and Centrin3 (centrosomes) in RPE1 cells. Arrows indicate centrioles; arrowheads denote centriolar satellites. Scale bars: 10 μm (2 μm for insets). **b,** Immunofluorescence images of LRCH2(red), Ace-tubulin(pink), CCDC22-mEmerald(green) and DAPI (nucleus, blue). Scale bars: 10 μm (1 μm for insets). **c,** Super-resolution microscopy (SIM) of endogenous CCDC22 relative to acetylated tubulin (Ace-tubulin), with corresponding top and side views. Scale bar, 0.4 μm. **d,** SIM of endogenous CCDC22 relative to C-NAP1. Scale bar, 0.4 μm. **e,** SIM of endogenous CCDC22 relative to glutamylated tubulin. Scale bar, 0.4 μm. **f,** SIM of endogenous CCDC22 relative to Centrin3. Scale bar, 0.4 μm. **g,** IP analysis

of LRCH2 and CCDC22 in RPE1 cells using an anti-CCDC22 antibody. **h,** Immunofluorescence images of cilia (Arl13b, yellow) and centrosome (Centrin3, blue) in WT, *LRCH2* KO cells, *CCDC22* KO cells and DKO cells. Scale bars: 20 μm (2 μm for insets). **i**, IP analysis of CCDC22 and LRCH2 after serum starvation. **j,** Quantification of LRCH2 enrichment in **i**, Data are presented as mean ± s.e.m.; n = 3 independent experiments. Statistical significance was assessed by one-way ANOVA with multiple comparisons.